AIAA JOURNAL
Vol. 44, No. 2, February 2006

Technical Notes

TECHNICAL NOTES are short manuscripts describing new developments or important results of a preliminary nature. These Notes should not exceed 2500 words (where a figure or table counts as 200 words). Following informal review by the Editors, they may be published within a few months of the date of receipt. Style requirements are the same as for regular contributions (see inside back cover).

Improved Prediction of Plane Transverse Jets in Supersonic Crossflows

A. T. Sriram* and Joseph Mathew†
Indian Institute of Science, Bangalore 560 012, India

Introduction

THE flowfield due to transverse injection of a round sonic jet into a supersonic flow is a configuration of interest in the design of supersonic combustors or thrust vector control of supersonic jets. The flow is also of fundamental interest because it presents separation from a smooth surface, embedded subsonic regions, curved shear layers, strong shocks, an unusual development of the injected jet into a kidney-shaped streamwise vortex pair, and a wake behind the jet. Although the geometry is simple, the flow is complex and is a good candidate for assessing the behavior of turbulence models for high-speed flow, beginning with the corresponding two-dimensional flow shown in Fig. 1. At the slot, an underexpanded sonic jet expands rapidly into the supersonic crossflow. Expansion waves reflect at the jet boundary, coalesce, and give rise to a Mach surface (Mach disk for round jets). The plane jet reattaches downstream. The jet is also an obstacle to the supersonic crossflow and generates a bow shock ahead. Consistently, the wall boundary layer is separated and the separation shock intersects the bow shock. Usually, four recirculation zones are found, termed primary upstream vortices, secondary upstream vortices, primary downstream vortices, and secondary downstream vortices.

Previous computations (discussed hereafter) agreed closely with experiments at low injection pressure ratios and differed noticeably as the injection pressure was increased. The distance to the upstream separation location was smaller in the computations, and the pressure rise in the separation region was higher. These differences can remain even as the grid is merely refined (for instance, doubled), rather than redistributed. We find that the solution can improve when the region from the wall up to at least the Mach surface is well resolved. As injection pressure is raised, the Mach surface moves away from the wall and is even outside the incoming boundary layer. A similar configuration is obtained when the slot width is larger (other parameters remaining the same). In both cases, when there is good resolution within the boundary layer and also outside, at least up to the Mach surface, the distance to the upstream separation location becomes very close to that in the experiment even though the overall pressure rise remains noticeably higher.

Presented as Paper 2004-1099 at the AIAA 42nd Aerospace Sciences Meeting, Reno, NV, 6–9 January 2004; received 11 April 2005; revision received 28 September 2005; accepted for publication 12 October 2005.

*Ph.D. Student, Department of Aerospace Engineering.
†Associate Professor, Department of Aerospace Engineering. Senior Member AIAA.

Data from three sets of experiments are available. The earliest experiments, from Spaid and Zukoski,[1] are of particular value because they were done systematically, cover a large range of injection pressure ratios, and provide good spatial resolution of the wall pressure data. Their precaution of using sidewalls (or end plates) to obtain a nearly two-dimensional flow has proved essential when good quality simulations are to be assessed. Actual loss of two-dimensionality at the highest freestream Mach number was documented as well. Recent data from Aso et al.,[2] corrected by Aso et al.,[3] are also available. Simulations of the experiments of Spaid and Zukoski[1] and the corrected ones of Aso et al.[3] are presented hereafter.

Computations

Favre-averaged Navier–Stokes equations, coupled with the two-equation (k–ω) turbulence model of Wilcox[4] (Secs. 4.3.1 and 5.3), were integrated to steady states. A compressibility correction employed by Wilcox[4] (Sec. 5.5) was incorporated in the k and ω equations. The equations were cast into a finite volume formulation. Roe's approximate Riemann solver was used to obtain inviscid fluxes after extrapolating the variables for higher-order spatial accuracy through MUSCL (second and third order); min-mod and Van Albada limiters were used to avoid spurious oscillations. Converged solutions with residues falling through several decades were obtained in all cases.

The code was developed and tested systematically by computing a standard, laminar inviscid, and viscous shock reflection problem, and a turbulent flat-plate boundary layer. Details are available elsewhere.[5,6] Figures showing convergence to a solution of the present problem with systematic grid refinement, first in one direction, then in the other, and the fall in residues through several orders, have been presented before.[6] Here, solutions with our code have been compared with those of other investigators in Figs. 2 and 3. Improvements were sought starting from these basic solutions.

The computational domain is a rectangle bounded by a no-slip, adiabatic wall. Grids are clustered in both directions. In the wall-normal direction the cell width is about one wall unit in the turbulent boundary layer ahead of the upstream separation point. For a case with 240 streamwise gridpoints, there are 23 points over the slot. The inflow is uniform and supersonic just ahead of the plate leading edge, and all quantities were specified. Pressure at the wall was extrapolated from the interior by setting the value at the wall equal to the value attained at the neighboring cell away from the wall. (The wall-normal derivative vanishes to first order.) At the slot the flow is sonic and issues normal to the plate; all quantities were specified

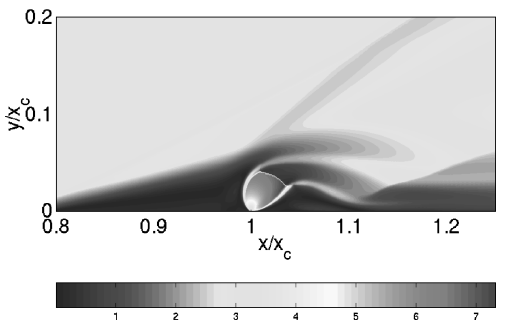

Fig. 1 Mach number distribution.

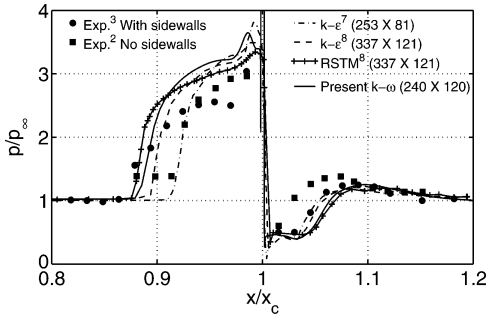

Fig. 2 Wall pressure distribution from several computations and experiments compared ($p_{\text{jet}}/p_\infty = 17.72$).

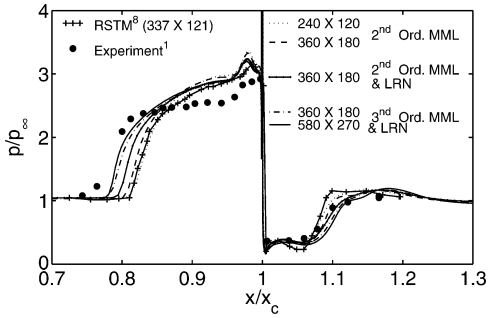

Fig. 3 Effect of strategies to improve the simulation of the Spaid and Zukoski[1] experiment: Second- and third-order schemes with min-mod limiter (MML) and low-Reynolds-number (LRN) correction; computation with RSTM by Chenault and Beran.[8]

at sonic conditions. Conditions at the upper and outflow boundaries were obtained by extrapolation, taking derivatives normal to the boundary to be zero to first order.

Turbulence quantities are also prescribed for the supersonic inflow and for the sonic jet. At inflow, k was specified taking turbulence intensity to be 0.5% [$k = 1.5(0.5U_\infty/100)^2$; freestream velocity is U_∞]; ω was then by obtained by taking eddy viscosity equal to fluid viscosity. Because of the turbulence evolution, the flow structure and especially the wall pressure, which is compared here, were not found to be sensitive to the inflow turbulence level. At the wall k was set to zero, and the hydraulically smooth-surface condition (Wilcox,[4] Sec. 4.7.2) was used to calculate ω ($\omega = 100u_\tau^2/\nu$ for friction velocity u_τ, kinematic viscosity ν, and roughness of five wall units). For the sonic jet, $k = 100\ \text{m}^2\text{s}^{-2}$ and $\omega = 5 \times 10^5\text{s}^{-1}$.

Results and Discussion

Widely Used Test Case

Previous reports of validations[7,8] were made of the experiments of Aso et al.[2] at freestream Mach number $M_\infty = 3.75$ and injection pressure ratio $p_{\text{jet}}/p_\infty = 17.72$ with the slot of width $w = 1$ mm at $x_c = 330$ mm from the plate leading edge. Rizzetta[7] applied the Jones–Launder k–ϵ model. Chenault and Beran[8] applied a Reynolds stress turbulence model (RSTM) derived by Zhang et al., as well as the k–ϵ model obtained by contraction. Our grid refinement study[6] of this case, with the second-order scheme and min-mod limiter, showed a grid of 240×120 to be adequate to obtain grid-independent solutions. Figure 2 shows wall pressure from present and previous computations compared with experimental data.[2,3] Present computations are close to the results derived by Chenault and Beran[8] and provide a good prediction of the upstream separation point. Other k–ϵ simulations are also shown in Fig. 2. The wall pressure distribution is a signature of some of the several flow features. The steep rise is due to the upstream separation shock, followed by a gradual rise over the separated flow, and a narrow peak at the shorter, secondary upstream vortex. Similarly, the downstream low-pressure well is over the primary vortex, with a narrower dip at the secondary vortex close to the slot. The pressure rise is the recovery at the recompression shock.

Figure 2 also shows the considerable effect of using sidewalls in the experiment. At the higher injection pressure ratio of 26.29, the upstream separation zone was 20 mm longer with side walls[3] than without them.[2] Solution characteristics are consistent across the various simulations: As the upstream separation length increases, the peak pressure decreases. The RSTM prediction is close to the better data, and the present k–ω prediction is of comparable accuracy.

Prediction of Highly Underexpanded Jet

In simulations reported so far, generally, accurate solutions have been found at low injection pressure ratios.[8] At higher levels all predictions degraded, including those with the sophisticated RSTM: The point of upstream separation lies closer to the injector, and the pressure rise is significantly larger. Figure 3 shows previous and present computations of a case from the experiments of Spaid and Zukoski[1] ($M_\infty = 3.5$ and $p_{\text{jet}}/p_\infty = 63.50$, their highest pressure ratio).

Initially, our calculations gave similar results.[6] Then, a series of systematic changes were made to obtain improved results. Grid refinement, to 360×180 cells, in itself provides only a slight improvement (Fig. 3). A low-Reynolds-number correction (Wilcox,[4] pp. 151 and 152) was found to have a beneficial effect (Fig. 3). Changing to third-order accuracy (with Van Albada limiter) showed further improvement. At this stage, further grid refinement to 580×270 cells showed little improvement. Primarily, the improvement has been in locating the upstream separation close to that in experiments. Peak pressure rise remains higher, as in previous computations. The downstream distribution comes even closer to experiment. Each improvement strategy provides for a higher-resolution solution of the initial portions of the jet up to the Mach surface (Fig. 1). Improved solutions show a continuous sonic surface from either side of the barrel shock and the Mach surface. At low injection pressures, the region up to the Mach surface lies within the incoming boundary layer and is usually well resolved. At higher pressures, as the Mach surface moves well outside this boundary layer, grid (or scheme) requirements change. Unless this portion of the jet is accurately captured, the jet boundary deflection is different and, due to the shallow upstream separation, the separation point moves considerably.

Simulation of Various Cases

For completeness, a summary of simulations of all of the available experiments is included here. The grid of 360×180 cells is used in all of the cases with the modifications mentioned earlier.

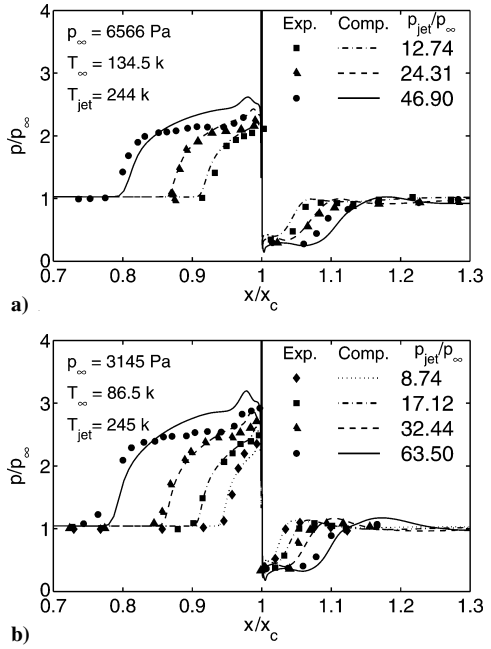

Fig. 4 Wall pressure comparisons with measurements of Spaid and Zukoski[1]: a) $M_\infty = 2.61$, $w = 0.2667$ mm, and $x_c = 228.6$ mm; and b) $M_\infty = 3.50$, $w = 0.2667$ mm, and $x_c = 228.6$ mm.

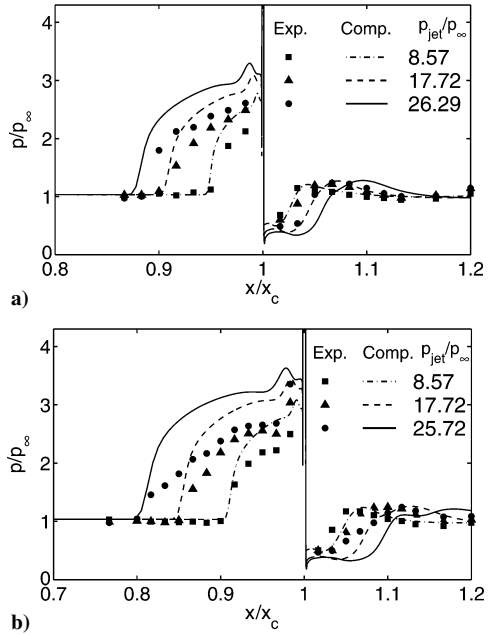

Fig. 5 Wall pressure comparisons with measurements of Aso et al.[3]: a) $M_\infty = 3.75$, $w = 0.5$ mm, and $x_c = 300$ mm; and b) $M_\infty = 3.75$, $w = 1.0$ mm, and $x_c = 300$ mm.

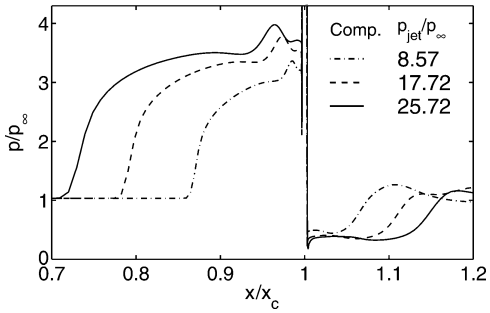

Fig. 6 Computed wall pressure for configuration in Aso et al.[3] with $M_\infty = 3.75$, $w = 2.0$ mm, and $x_c = 330$ mm.

Simulations of Experiments of Spaid and Zukoski

The experiments of Spaid and Zukoski[1] is of greater value because the many measurements near the slot provide good spatial resolution, sidewalls ensured two dimensionality (clearly documented), and the range of injection pressure ratio is large. The upstream pressure rise was steep, indicating separation of a turbulent boundary layer. Hence, truly two-dimensional, turbulent conditions prevailed. Computed wall pressure distributions (Figs. 4a and 4b) show good agreement with experimental data in all cases. The pressure plateau becomes clearer at higher injection pressures.

Aso et al.[3]

Aso et al.[3] reported wall pressures for two slot widths $w = 0.5$ and 1 mm and six injection pressures with $M_\infty = 3.75$, $p_\infty = 11090$ Pa, $T_\infty = 78.43$ K, and $T_{jet} = 245$ K. Computed and experimental wall pressures are shown in Figs. 5a and 5b. (For clarity, only alternate cases, including the maximum pressures, are plotted.) A close agreement on the upstream separation point was obtained, but there is a considerable discrepancy in the shape of the pressure profile, becoming more evident with increasing injection pressures. The sharp increase in pressure, characteristic of turbulent separation, was not found in the experiment, particularly at higher injection pressure. New experiments by, for example, tripping the inflow boundary layer may be useful.

Numerical Experiments

Three other simulations were performed with the slot width increased to 2 mm and $x_c = 330$ mm. Appropriate changes to the grid were made because the Mach surface is now located farther away from the wall. Computed wall pressures are shown in Fig. 6. Aso et al.[2] conducted experiments without side walls for this case but provided only upstream separation lengths (no wall pressure distribution). At the highest injection pressure, the measured[2] upstream separation length was about 50 mm. A previous computation on a relatively coarse grid[7] was about 66 mm. The present simulations give a solution of about 94 mm. Both careful experiments, in this case with sidewalls, and good numerical resolution are necessary. New experiments would allow more meaningful extensions to this assessment.

Conclusions

Numerical simulations of the flow due to injection of sonic jets into supersonic crossflows have been performed. Attention was focused on a particular case for which the earlier predictions had been poor. Improvement in prediction of the upstream separation location was demonstrated with higher-order formulas and known turbulence model corrections. As injection pressure increases, or a wider slot is used, all other conditions remaining the same, it was found necessary to have adequate resolution of the boundary layer as well as the region up to the Mach surface. Then, presently available Reynolds-averaged Navier–Stokes solutions are accurate over the full range of experiments considered, even though these flows are quite complex.

References

[1]Spaid, F. W., and Zukoski, E. E., "Study of the Interaction of Gaseous Jets from Transverse Slots with Supersonic External Flows," *AIAA Journal*, Vol. 6, No. 2, 1968, pp. 205–212.

[2]Aso, S., Okuyama, S., Kawai, M., and Ando, Y., "Experimental Study on the Mixing Phenomena in Supersonic Flows with Slot Injection," AIAA Paper 91-0016, Jan. 1991.

[3]Aso, S., Okuyama, S., Ando, Y., and Fujimori, T., "Two-Dimensional and Three-Dimensional Mixing Flowfields in Supersonic Flow Induced by Injected Secondary Flows Through Tranverse Slot and Circular Nozzle," AIAA Paper 93-0489, Jan. 1993.

[4]Wilcox, D. C., *Turbulence Modeling for CFD*, DCW Industries, Inc., La Cañada, CA, 1993, Secs. 4.3.1, 4.7.2, 5.3, and 5.5.

[5]Sriram, A. T., "Numerical Simulations of Transverse Injection of Plane and Circular, Sonic Jets into Turbulent, Supersonic Crossflows," Ph.D. Dissertation, Dept. of Aerospace Engineering, Indian Inst. of Science, Bangalore, India, 2003.

[6]Sriram, A. T., and Mathew, J., "Numerical Prediction of Two-Dimensional Transverse Injection Flows," AIAA Paper 2004-1099, Jan. 2004.

[7]Rizzetta, D. P., "Numerical Simulation of Slot Injection into a Turbulent Supersonic Stream," *AIAA Journal*, Vol. 30, No. 10, 1992, pp. 2434–2439.

[8]Chenault, C., and Beran, P. S., "K–ϵ and Reynolds Stress Turbulence Model Comparisons for Two-Dimensional Flows," *AIAA Journal*, Vol. 36, No. 8, 1998, pp. 1401–1412.

P. Givi
Associate Editor